NEW OBSERVATIONS ON

FLAGELLAR FINE STRUCTURE

The Relationship Between Matrix Structure and

the Microtubule Component of the Axoneme

FRED D. WARNER

From the Whitman Laboratory, Department of Biology, The University of Chicago, Chicago, Illinois. Dr. Warner's present address is the Department of Biology, Kline Biology Tower, Yale University, New Haven, Connecticut 06520

ABSTRACT

The sperm flagella of the blowfly *Sarcophaga bullata* demonstrate the relationship of radial projections in the matrix region to the microtubule organization of the axoneme. The A microtubule of each peripheral doublet is connected to the central sheath by a series of paired radial links. The links lie along the tubule wall with a alternate spacing of about 320/560 A. The distal end of each link is enlarged into a globular head that connects via a transitional link to the helical sheath around the central microtubules. The radial link pairs are disposed in the form of a double helix with a pitch of about 1760 A. It is proposed that a similar organization is common to all cilia and flagella showing ninefold symmetry and must provide, in part, the morphological basis for motility.

INTRODUCTION

Numerous fine structure studies have demonstrated the unambiguous nature of microtubule organization in eukaryotic cilia and flagella. With the known exceptions of sciarid (23) and coccid (27) insect sperm, the motile organelle consists of microtubules arranged in a circular profile showing ninefold rotational symmetry. Most commonly, this profile is formed by tubules in $(9) + 9 + 2$, $(9) + 9 + 1_n$ or $(9) + 9 + 0$ arrays. Accordingly, proposed models for the mechanism of ciliary motility have been directed to this tubule component. The problems attendant with such models are treated at length in reviews by Brokaw (7), Holwill (37), and Sleigh (33). However, Satir's (30) elegant demonstration that the doublet microtubules do not measurably contract, but slide during stroke formation, neces-sarily directs attention to the possibility of other components being actively related to bending of the flagellar shaft.

Early studies of ciliary fine structure (1, 4, 11, 12) indicate the presence of fibrous structures lying in the matrix area between central and peripheral microtubules. Afzelius (1) first described a set of nine "spokes" between the two groups of tubules in sea urchin sperm. Gibbons and Grimstone (11) initially observed nine longitudinal "secondary fibers" lying midway between the two tubule groups. Gibbons later determined (12) that these were connected to a sheath around the central tubules and to the A microtubule of each peripheral doublet by a series of nine radial links, equivalent to the "spokes" of Afzelius. Manton and Clarke (19) were the first to deduce

helical organization of matrix structures, and this has been recently confirmed by Paolillo (21) in a study of *Sphagnum* sperm flagella. Matrix structure was generally thought to be important for structural stability of the axoneme, although André (4) suggested an active role for the "secondary fibers" in the motile process.

However, all previous studies remain inconclusive as to the precise structure and organization of these elements, owing to their variable retention after fixation for electron microscopy. Hence, an accurate model of microtubule-matrix organization is lacking and thus has impeded elucidation of both the morphological and biochemical bases of motility. In the present study, the sperm flagella of a dipteran were examined in order to ascertain the fine structure of matrix elements and, in particular, their relationship to the axoneme microtubules. Although insect sperm flagella often have accessory structures lying outside the doublet microtubule profile, they appear to share a basic structural pattern in common with all motile cilia and flagella. This pattern consists of an axial unit of microtubules and/or helically wound fibers joined by radial linkage to the nine peripheral doublets. The structural model that is here proposed is based on the inactive flagellum of the mature spermatid and will serve as a basis for further study of the motile process.

MATERIALS AND METHODS

Whole testes from 12-day pupae of *Sarcophaga bullata* (Parker) were fixed for 2.5 hr in 4% glutaraldehyde (Polysciences, Inc., Warrington, Pa.) buffered at pH 7.4 with 0.1 M *s*-collidine (Ladd Research Ind., Inc., Burlington, Vermont). Tissue was then washed for 30 min in the buffer and postfixed in collidine-buffered 2% OsO_4 for 45 min. All fixation procedures were done at 4°C. Following postfixation, tissue was rapidly dehydrated in ethanol series, treated briefly with propylene oxide, and embedded in Epon 812.

Dark-gray interference-color sections cut on a diamond knife were used exclusively in this study. Sections were stained for 15 min in 5% aqueous uranyl acetate followed by 1 min in Reynolds' lead citrate and examined in an RCA EMU-4A electron microscope operated at 50 kv. All plates were exposed at original magnifications of $\times$ 25–50,000 and subsequently calibrated to less than 5% magnification error by using carbon-grating replicas.

Negatively stained preparations were made according to the following procedure: Whole testes were teased apart in a drop of 1% aqueous phosphotungstic

acid (PTA) adjusted to pH 7.2 with NaOH. A carbon-coated grid was touched to the surface of this preparation, excess fluid was removed with bibulous paper, and the remaining film was allowed to air dry. Total staining time was ca. 5 min at room temperature. The preparations were examined at 100 kv and plates were exposed at magnifications of $\times$ 50–100,000.

In order to enhance the symmetrical and periodic structure inherent in the axoneme, both rotational ($360°/n; n = 9$) and translational (inherent period x 6 translations) image reinforcement techniques were used. On the final photographic enlargements, measurements of less that 1000 A (ca. 15 mm) were made with an optical comparator fitted with a 0.1 mm division scale. Angular determinations were made with a 360° scale fitted to the comparator.

RESULTS

A Note on the Figures and Terminology

The term *axoneme* is used in lieu of "axial filament complex" and includes all components limited by the accessory microtubules and coarse fibers. Hence, membranous and mitochondrial structures are omitted. The term *microtubule* or *tubule* is used in contradistinction to the terms "fiber" and "filament" that appear in the literature. *Median sagittal* denotes the plane bisecting the aligned centers of both central microtubules.

All transverse sections of flagella are viewed from flagellar base to tip (doublet skewing and arms directed clockwise). Accordingly, the microtubule numbering system of Afzelius (1) is used. Doublet No. 1 lies perpendicular to the central tubule plane as it passes between tubules (Fig. 6), and numbering then proceeds in the direction of arm attachment to the A tubule of the doublet. Doublet No. 3 thus lies in the same plane as the central tubules. Some position variability is inherent in doublet placement, but the presence of additional markers makes it reliable for this system. The narrow x side of the asymmetric central sheath is always disposed towards the No. 1 doublet to which it connects via radial projections. In addition, the constant position of the mitochondrial crystalloids and the central tubule plane allow doublet numbering in most longitudinal sections. Because of these markers, all structures lying in ninefold rotational symmetry can be numbered in parallel with the doublet numbering method.

All electron micrographs are from unbent or nearly straight regions of the axoneme. This is taken to represent the inactive state of the flagel-

lum, particularly since the spermatids are non-motile though structurally mature in 12-day pupae. However, the flagella do undergo several passive bends within the testes. The black-on-white calibration bar applied to most figures represents a span of 1000 A, unless otherwise noted. The diagram insert in most longitudinal sections indicates the section plane and approximate area encompassed by both plane and section thickness.

The linear periodicities present in most longitudinal sections can be visually enhanced if the viewer looks down the axis of the figure from an eye angle of approximately 15° to the plate surface.

General Description of the Flagellum

The fine structure and morphogenesis of the blowfly spermatid is presented in detail in another paper.[1] Typically, the mature spermatids lie in numerous bundles, each containing 128 spermatids, within the testes (Fig. 1). The area between adjacent spermatids is filled by densely packed, tubular structures (Fig. 2). Included in the flagellar structure are the two dense crystalloids of the mitochondrial derivatives (Fig. 2). The crystalloids are separated by a noncrystalline third element along much of their length (Fig. 1, inset).

The flagellar axoneme has the nine-single, nine-double, two-single microtubule organization typical of many insect sperm. The axoneme is approximately 1 mm long, 0.25 μ in diameter, and is limited by the circular profile of nine single or accessory microtubules. Each accessory tubule forms from a short projection off the B tubule of the doublet[1] and hence can be numbered in parallel with the doublets (Fig. 6). In addition, there is a suggestion of linkage between the accessory and B tubules in the mature spermatid (Figs. 2–5). Laterally adjacent to each accessory tubule are two dense fibers, termed coarse fibers, that extend the length of the axoneme. The more prominent of the two bears five short, 60 A centrifugally pointing projections so that the fiber appears crownlike in transverse section (Figs. 2, 6). This structure is more readily apparent in the rotation image (Fig. 3). It is not clear if the two coarse fibers are themselves joined or if they are

---

[1] F. D. Warner. 1970. Submitted for publication.

linked to adjacent accessory and doublet tubules. Both normal and rotation images show indications of such linkage (Figs. 2–5). The fibers are depicted as separate in Fig. 6.

Centripetal to the profile of accessory tubules and coarse fibers lie the nine sets of doublet microtubules. The circular profile of doublets has an outside diameter of 0.21 μ. The doublets are characteristically skewed clockwise at a pitch of 10–15° when viewed from flagellar base to tip (Figs. 2–6), as initially defined by Gibbons and Grimstone (11). The A tubule of each doublet lies innermost along this angle and appears somewhat smaller than the apposed B tubule. Both are compressed such that they appear ellipsoidal in transsection, and the wall between them appears doubly thick. The A tubule bears the paired arms. In transsection, the arms show a characteristic bend inward and, in addition, the end of the outer arm displays the prominent "hook" configuration (2). Arm structure is more clearly revealed in the rotation images (Figs. 3–5). In longitudinal section, the arms are spaced at regular intervals of 200–220 A along the tubule (Fig. 17) and appear to be about 110 A thick. The distal region of the arms appears bent in this plane as well, although this may result from superimposition of the two due to section thickness. The arms do not appear to link directly with the adjacent doublet although there is a suggestion of a faint strand connecting the inner arm with the B tubule in transverse sections.

Each doublet is joined by radial projections across the axoneme matrix to the sheath surrounding the central microtubules. This situation is described in detail below. The two central tubules, as well as the nine accessory tubules, each have a diameter of 300 A and wall thickness of 85 A. In the center of each tubule lies a "hollow" 70 A filament similar in appearance to the subunits of the tubule wall (Figs. 1, 2).

Central Sheath

Surrounding the two central microtubules is the central sheath. Viewed in transverse section, the sheath is seen as a moderately electron-opaque region with a generally circular profile of 700 A diameter (Figs. 1, 2). The sheath lies on both sides of the plane through the central tubules, although it is not clear that it encompasses the lateral edges of both tubules (see below). The sheath has an asymmetric, translucent central
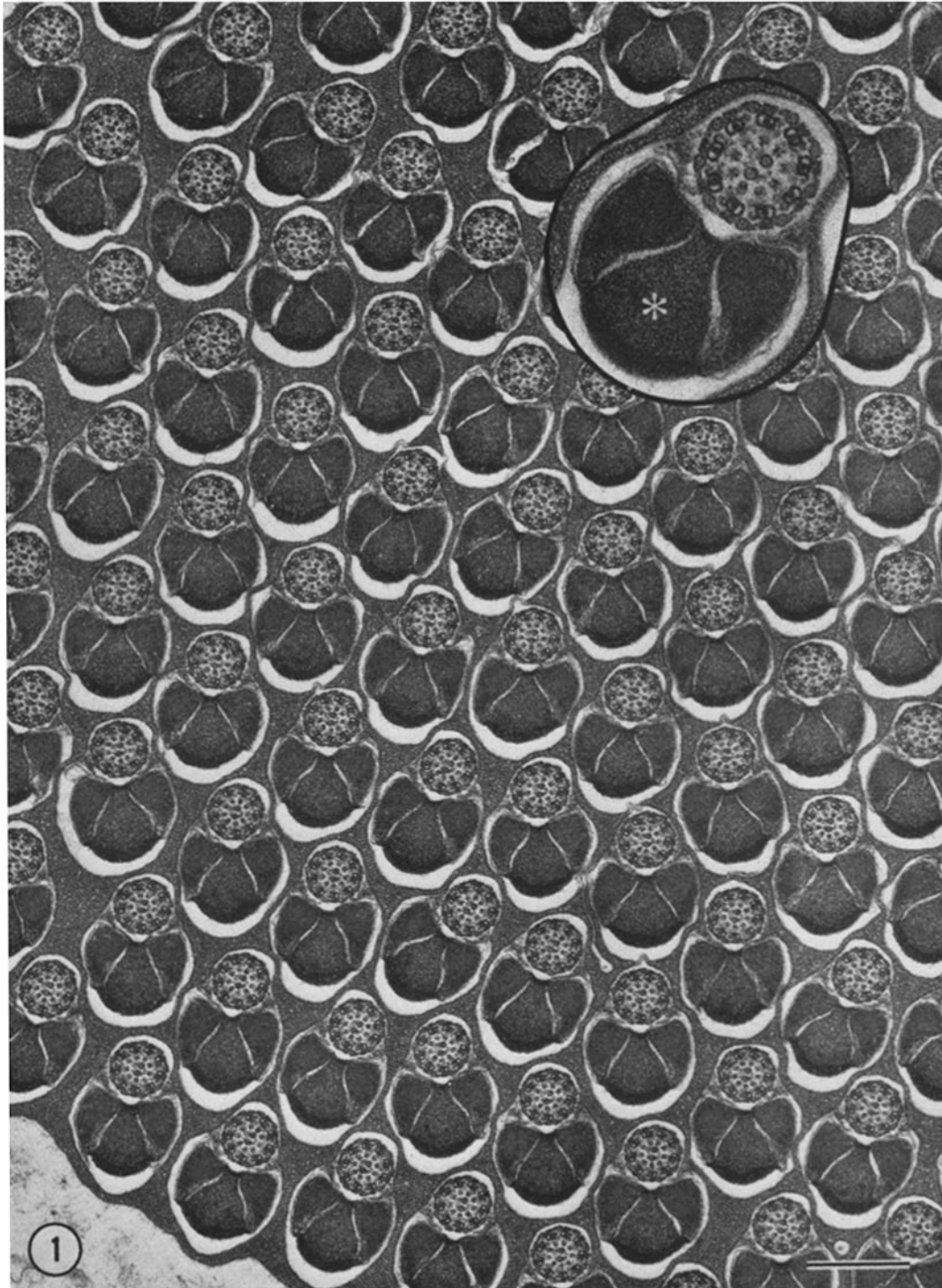
FIGURE 1 Low-magnification view of a transversely sectioned sperm bundle. Flagella are closely packed and similarly oriented. The calibration bar represents 0.5 μ. $\times$ 30,000. The *inset* shows a single flagellum and its two mitochondrial derivatives separated by a third element (*). $\times$ 75,000.
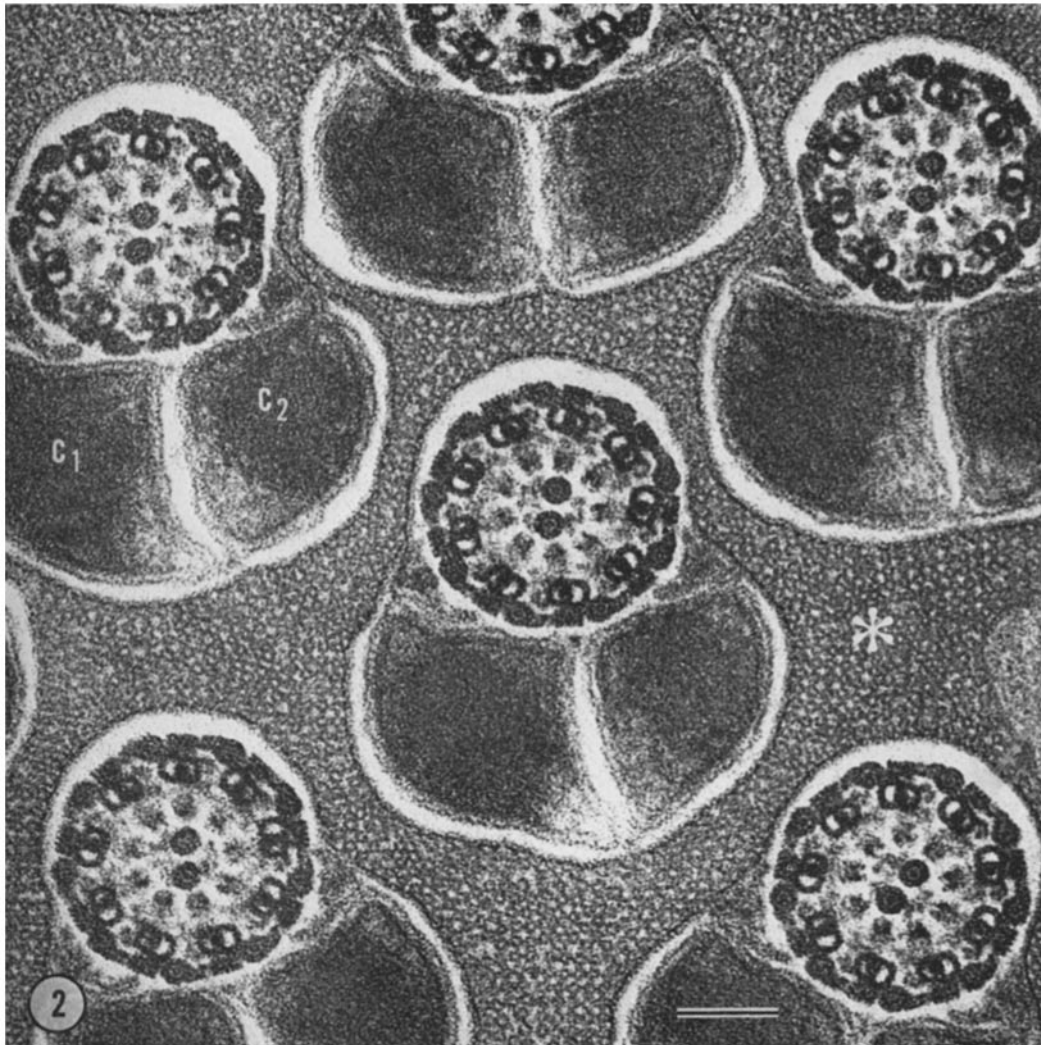
FIGURE 2 High-magnification view of several flagella, transversely sectioned near the tip. Each flagellum is surrounded by densely packed, tubular structures (*), and the mitochondrial derivatives (C_1, C_2) lack the third element at this level. Refer to Fig. 6 for a key to the axoneme structures. $\times$ 135,000.

region such that the sheath side directed toward the No. 1 doublet appears as a narrow, 150 A wide arc (arbitrarily termed x). On the opposite side of the tubules, the sheath is wider (termed y) and thus bridges a portion of the 90 A space separating the two tubules (Figs. 2, 6).

Viewed in longitudinal section (Fig. 9) the sheath is visible as a series of parallel cross-striations tilted consistently at an 8–10° angle. The electron-opaque striations are each 60 A wide and spaced 160 A center-to-center. Figs. 7 and 8 show a continuous section which moves from

sheath surface x to surface y. The x surface shows 160 A striations superimposed over the surface of both central tubules (Fig. 7, bottom). The striations are tilted at 10° from right-to-left and are in register, even though no cross-bridging occurs between the tubules, owing to the asymmetric central region mentioned above. As the section plane moves to the y surface (Fig. 7, top), the striations begin to bridge the gap between tubules and still lie in register, superimposed over the tubule surfaces. However, at this point, the angle of inclination has reversed itself, indicating that
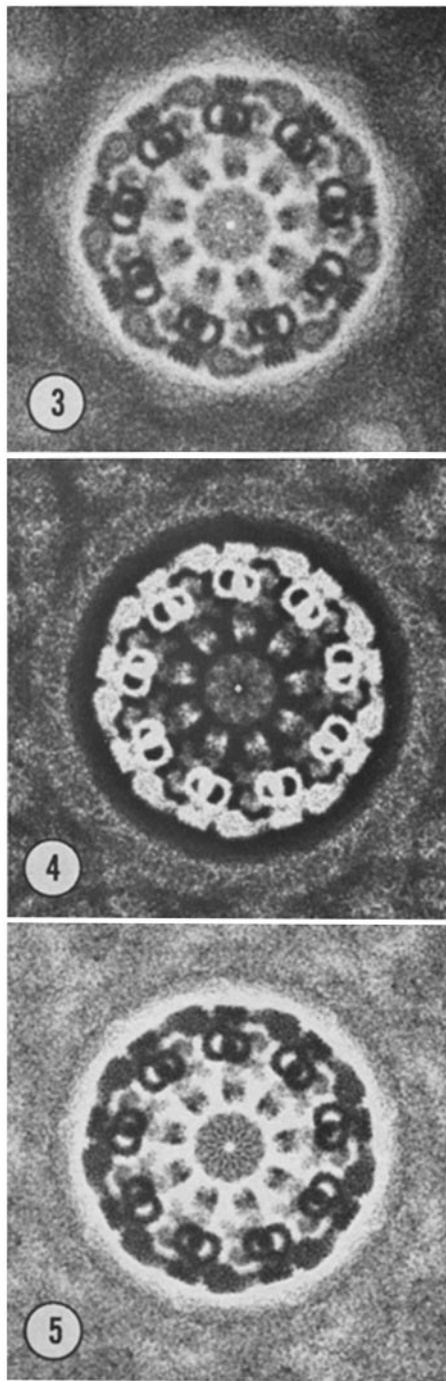
the striations are helically disposed around the central tubules. By virtue of its 160 A period and 8–10° inclination, the helix must be considered as single-stranded. It also appears to be a left-handed helix, although this was not firmly established. In Fig. 8, the striations are still visible as the section plane begins to include the radial link heads (top of figure) to be described. However, the striations are not so uniformly inclined as is usual and may vary between 0 and 10°, although the period remains constant.

At the central tubule surface opposed to the transitional links from doublet Nos. 3, 7, or 8, the 160 A striations appear to extend approximately 25 A past the lateral edges of the tubules in the central pair plane (Figs. 7, 11). Fig. 10 shows a surface section of the sheath that includes one central tubule such that its lateral edge is facing the viewer. The tubule is indistinct, yet 160 A striations span it and join in register with the prominent sheath period on the left and right (x and y). It is apparent that the sheath striations are disposed at two angles. It is not possible, with sectioned material, to determine whether we are, indeed, dealing with an inherent 160 A helical period of the microtubule wall and a separate 160 A helical period of the actual central sheath, although this is suggested. However, the striations appear to be in angular and periodic register between the sheath and tubule wall. In Fig. 13, approximately five longitudinal striations, each showing a 50 A center-to-center period, are occasionally visible in the tubule wall. Transversely superimposed over this is the 160 A period.

Radial Links

Midway between the peripheral doublets and central sheath lies a ring of nine dense "granules," each of which is joined to an adjacent doublet in the same sector of ninefold symmetry (Figs. 1, 2). These granules are the distal ends or *link heads* of the *radial links* connecting to the doublet. In axoneme transsection, the head is not uniformly opaque but appears to have a substructure of two laterally opposed dense regions so that it appears as a blunt, two-pronged "fork" directed to the sheath (Figs. 2–6). The heads are about 200 A

FIGURES 3–5 Rotation images ($n = 9$) processed from sections at three levels of the axoneme. $\times$ 144,000.
FIGURE 3 Section near the flagellar base. The crownlike coarse fibers are particularly clear.
FIGURE 4 Section from the flagellar midregion, similar

to those in Fig. 1. Negative image rotated from a positive projection plate.
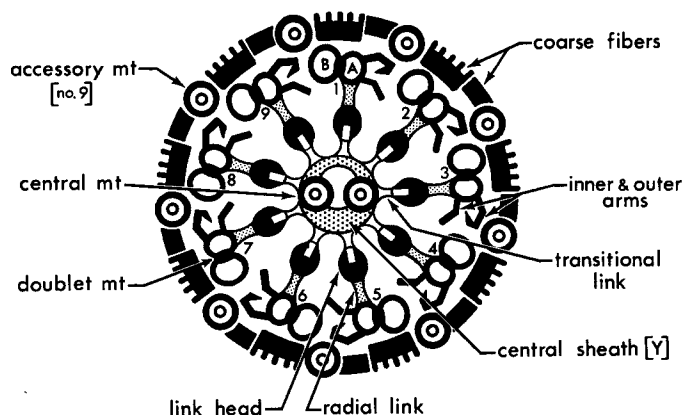FIGURE 5 Section near the flagellar tip, similar to those in Fig. 2.

FIGURE 6   Diagram of the flagellar axoneme as viewed in transverse section. The wide portion of the central sheath is indicated as Y, while the opposed narrow portion is termed X. The X side is always linked to the A tubule of the No. 1 doublet via the radial link. The link heads and transitional links as drawn should be taken to indicate only that substructure is present. Drawn approximately to scale.

wide and 280 A deep, and each lies 275 A centripetal to the surface of the doublet A tubule to which it is connected by the radial link. This is shown clearly by the rotationally enhanced mages (Figs. 3–5). There are no lateral connections between adjacent heads.

In median sagittal section the link heads along the Nos. 3 and 8 doublets are visible as 280 A globular units on opposed sides of the axoneme (Figs. 11–13). The radial links are obscured because of the presence of amorphous electron-opaque material surrounding adjacent links. The heads are arranged in longitudinal pairs and show an alternate center-to-center spacing of about 320/560 A or occasionally 320/640 A. Fig. 12 is a linear translation of the previous figure (6 x the 560 A period) and reveals the paired heads quite distinctly. If the longitudinal section is peripheral so that two or three adjacent head rows are included (Figs. 14, 15), the heads' paired spacing is still clear. In this view, the heads are 200 A wide and 280 A long, rather than globular as in median section, and each again appears as two laterally opposed dense regions which reflects their structure as viewed in trans-section. Head pairs of adjacent rows always line up at parallel inclination angles of 25–55° (Figs. 14, 15) and never appear in horizontal register. Since this angular alignment is always observed in peripheral sections and can be superimposed on median sections (Fig. 12), this must be regarded as firm evidence that the link heads (and links) are helically disposed in the flagellar matrix.

In view of the 320/560 A spacing and thus 880 A period of the radial links and heads, as well as additional evidence presented below, the helix must be regarded as double with helically adjacent link pairs forming each strand. Four and one-half successive pair displacements of 196 A, or an approximate half-turn of the helix, equal 880 A or the helix period as seen in median section. The pitch is thus 1760 A (Fig. 18). However, it is apparent in Figs. 11 and 12, and depicted in Fig. 18, that the link pairs on opposite sides of the axoneme are not in horizontal register. There has been a displacement which generally varies between 160 and 440 A but is depicted as (*200 A) in Fig. 18. Because of this displacement, the helix inclination angles are not symmetrical; that is, a 200 A displacement results in a helix with alternating half-turn angles of approximately 35° and 45°. This is diagrammed in Fig. 18 and is interpreted as resulting from doublet sliding distortion owing to nearby flagellar bending (see Discussion). If the spacing, period, and pitch of the radial links are constant (and research in progress indicates that this is so), a true helix pitch angle of 40° can be predicted for the link head site. Two other choices are possible, given the spacing and period: a single-strand helix with a pitch angle of about 30° (440 A half-turn displacement necessary), or a double-strand helix with a pitch angle of about 60°. However, the observed range of 25–55° angular distortion in peripheral sections suggests that the true helical conformation of radial link heads is double with a pitch angle of 40°. Helical
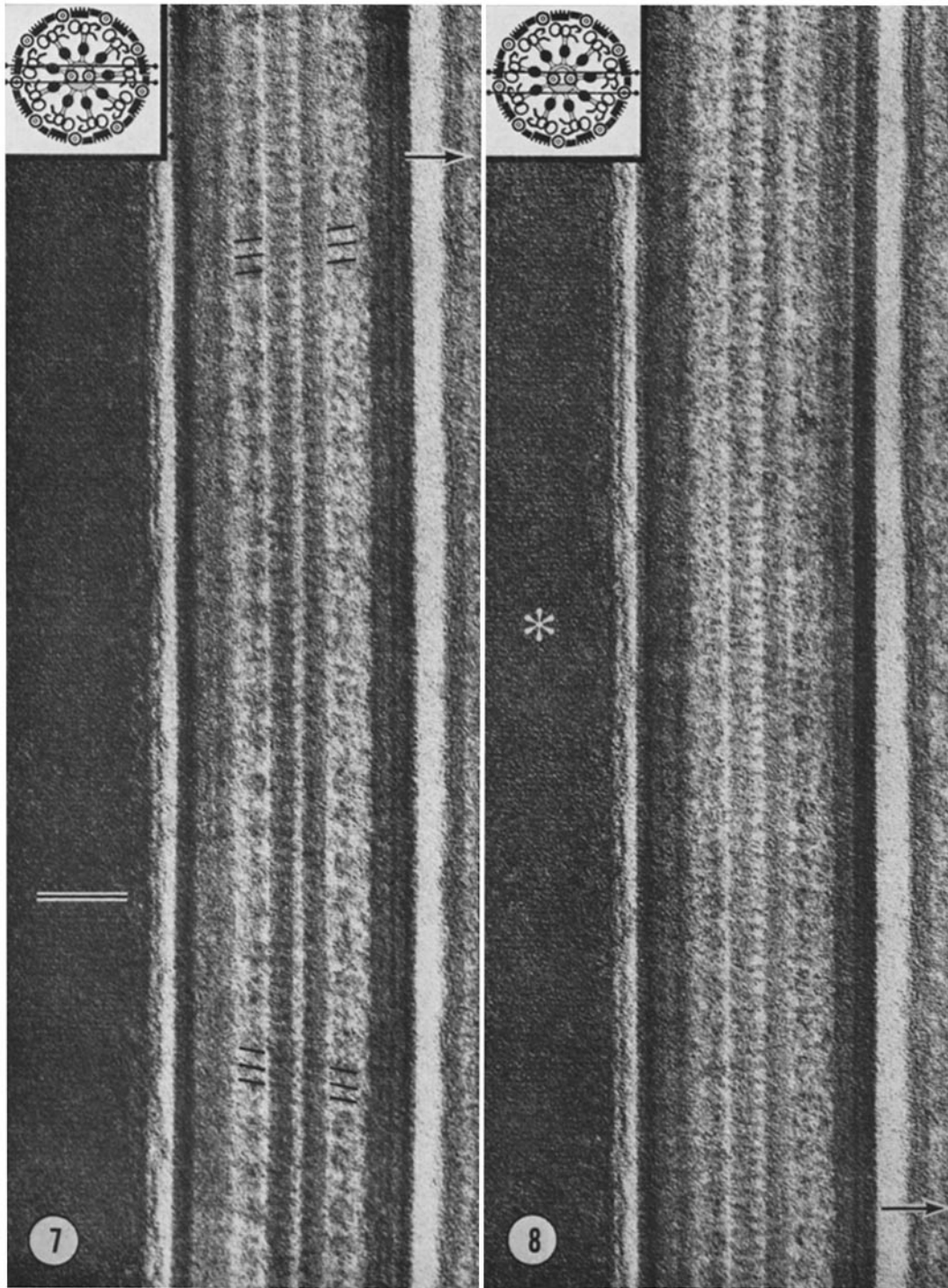
FIGURES 7 and 8 Continuous median sagittal section through a single flagellum covering a distance of about 3 μ. The horizontal arrows indicate the points of figure overlap. One of the mitochondrial crystalloids showing a minor period of 62 A lies to the left of each figure (*). × 135,000.

FIGURE 7 Transverse striations (x sheath-side) are visible over both central tubules (lines), inclined left-to-right (bottom). As the section plane moves to the y sheath-side (top), the striations reverse inclination and begin to bridge the gap between tubules.

FIGURE 8 Section plane is completely on the y sheath-side, and striation bridging between tubules is consistent.

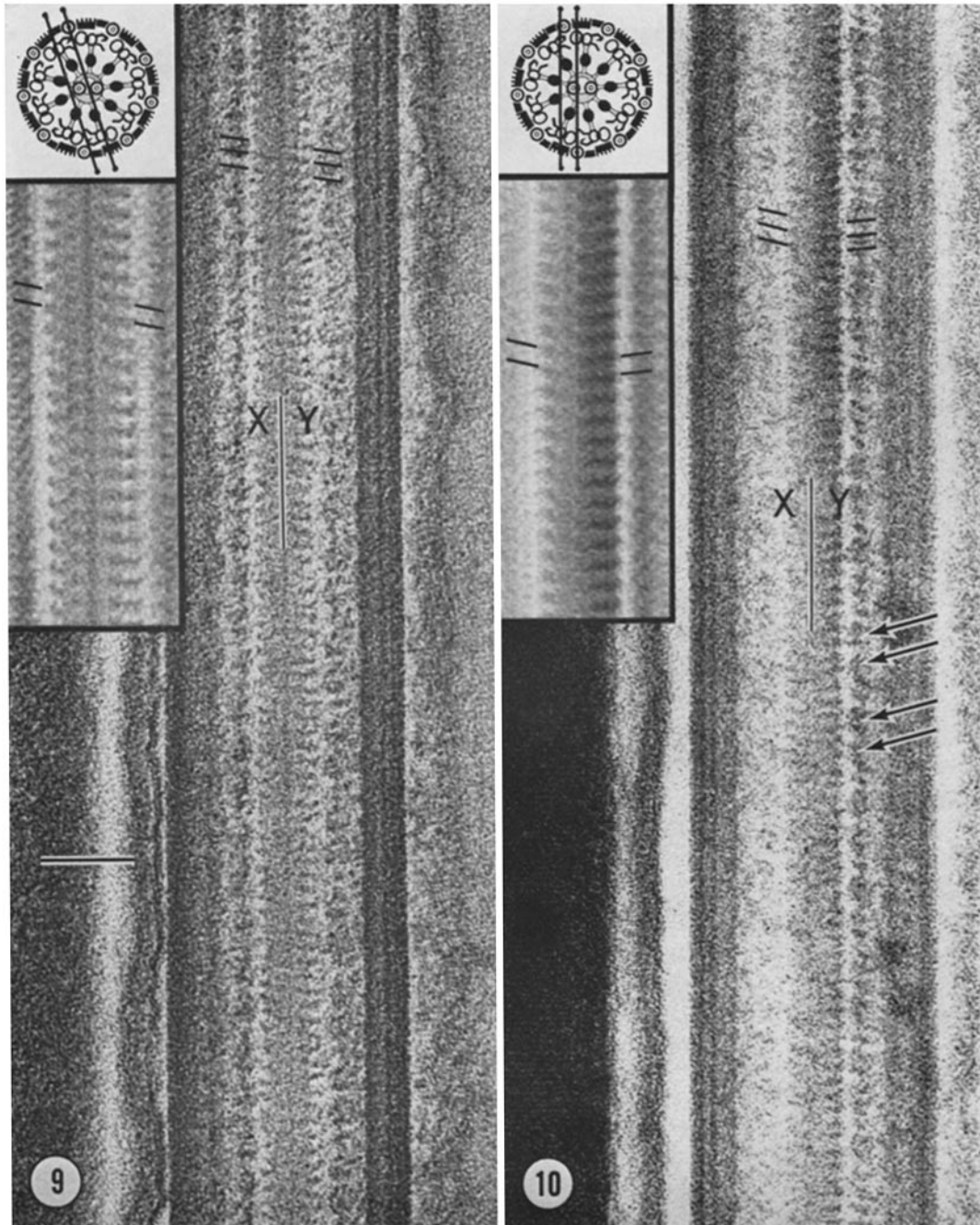FIGURE 9   Central sheath striations are visible in this plane but are most clear on the y sheath-side. × 135,000. The *insert* is a linear translation (6 *x*) of a portion of the sheath and shows the 160 A period and ca. 10° inclination. × 200,000.

FIGURE 10   Surface section of the sheath showing both the x and y sides meeting from different inclinations (lines). The arrows denote regions of junction between the radial link heads and the sheath striations. × 135,000. The *insert* is a linear translation (6 *x*) showing the period and two inclination angles. × 200,000.

FIGURE 11   Median sagittal section showing a row of radial link heads adjoining the No. 8 doublet (right arrow) and a second row adjoining the No. 3 doublet (left arrow). No regular cross-bridging is visible between the central tubules (*MT*). $\times$ 135,000.

FIGURE 12   Linear translation (6 x) of the previous figure. The paired link heads along the doublets are quite clear and their double helical configuration is drawn in at the top of the figure. Note that the head pairs are out of register by about 200 A on opposite sides of the axoneme (horizontal line). $\times$ 144,000.
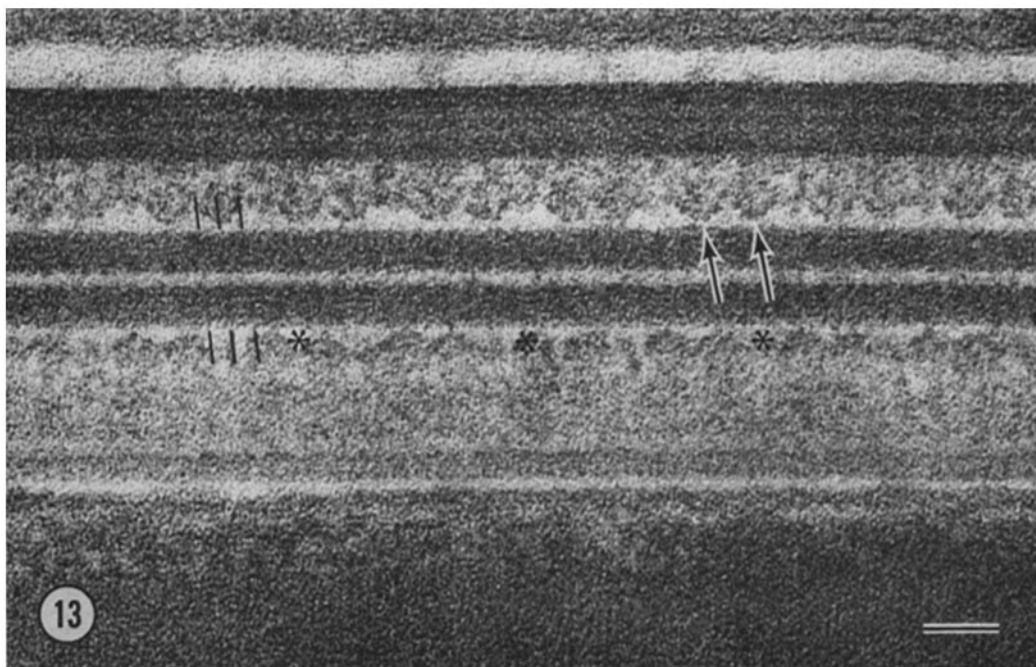
FIGURE 13   High-magnification view of the central pair tubules and adjacent link head pairs (arrows). Regions of the tubule wall showing longitudinal, 50 A striations are indicated by (*). Occasional transverse, 160 A striations are also visible (lines). The calibration bar represents 500 A. × 200,000.

conformation also lies at the radial link–microtubule wall junction. At this site, the pitch angle will be about 30°, since the helix radius has been increased without altering the link spacing. Both the link head site (40°) and the link-microtubule site (30°) are diagrammed in Fig. 18. However, in spermatid material it is convenient to view the link head position.

As noted earlier, the radial links are not clearly visible in median section. However, a peripheral section passing between link heads and doublets reveals the links transversely sectioned (Fig. 16). They lie with the same 320/560 A or 320/640 A spacing as the heads, and each has a diameter of 100–125 A. The radial links are seen most clearly in PTA negatively stained preparations. Fig. 19 shows four sets of doublet microtubules lying such that the A and B tubules are superimposed. The links project perpendicularly from the tubule (A) surface where they are spaced at 320/560 A or 320/640 A (Fig. 20). This characteristic spacing eliminates the possibility of their being confused with the arms that also lie along the A tubule, but which are not preserved in these preparations.

Not all links are perpendicular to the tubule surface, which indicates that there may be some flexibility at the link-tubule junction. As viewed in Fig. 20, each link is about 325 A long and 70–125 A thick. Thickness variation is probably due to the degree of flattening accruing during preparation. The length of each link suggests that the links must extend well into the head region since they are only about 275 A long when viewed in sectioned material. The links appear to consist of globular subunits (Fig. 20), although their organization is not clear. The distal end of each link appears to have some globular material adhering to it; in preparations less dispersed, considerable material remains attached (Fig. 22) which is undoubtedly the globular link head seen in thin-sections.

Link structure is not always so clear as is illustrated in Figs. 19 and 20. Fig. 21 shows four collapsed doublets that have twisted so that both the A and B tubules are visible along much of their length. The links are generally obscured, although they are clear in regions in which the doublet nature is less prominent. The inset in this figure
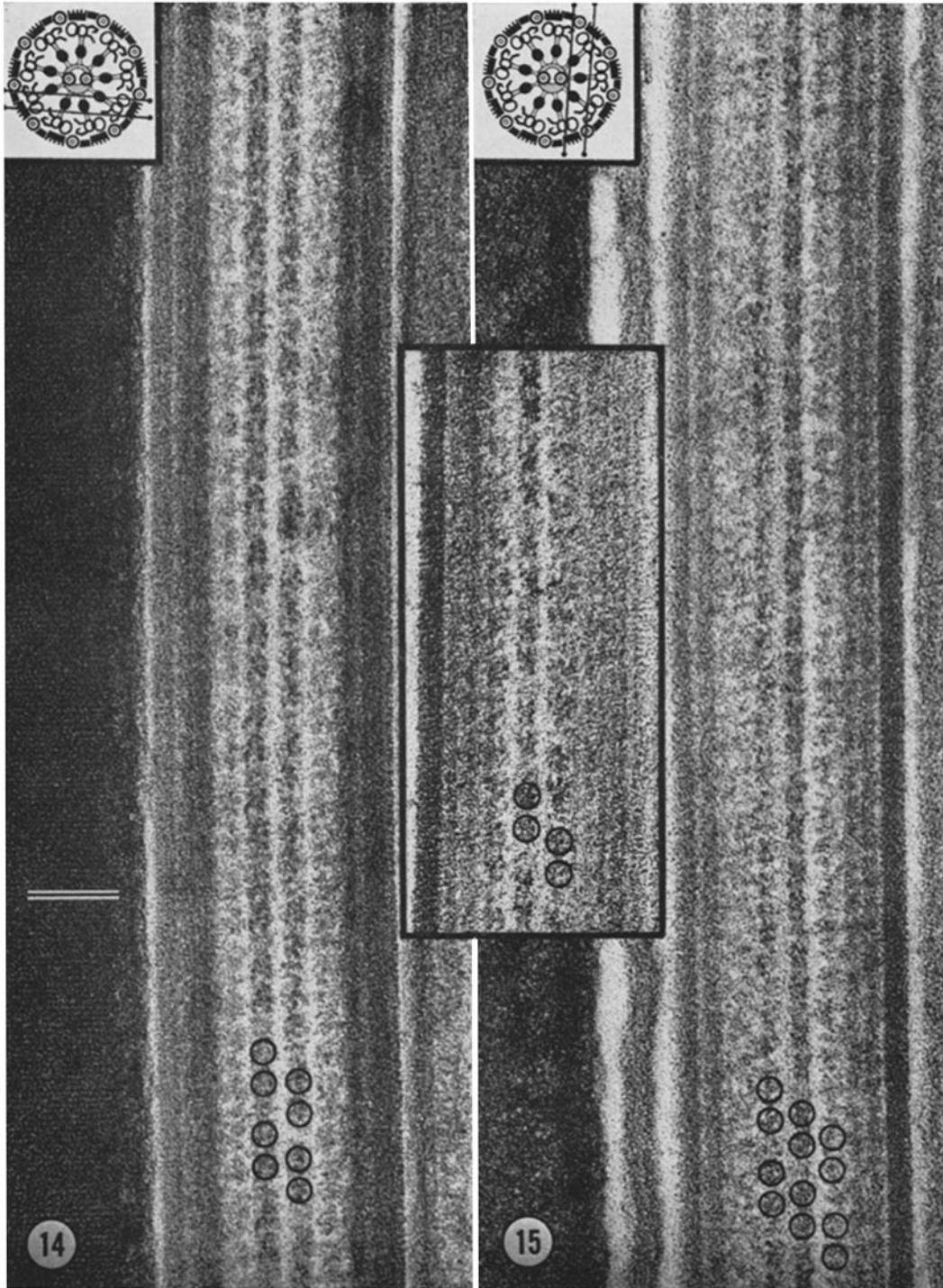
FIGURES 14 and 15   Peripheral sections showing two (Fig. 14) and three (Fig. 15) rows of radial link heads. Several pairs are circled and show their angular inclination varying between 35 and 45° in these figures. The *insert* shows head pairs in 55° alignment or a displacement of 440 A. All figures, × 135,000.
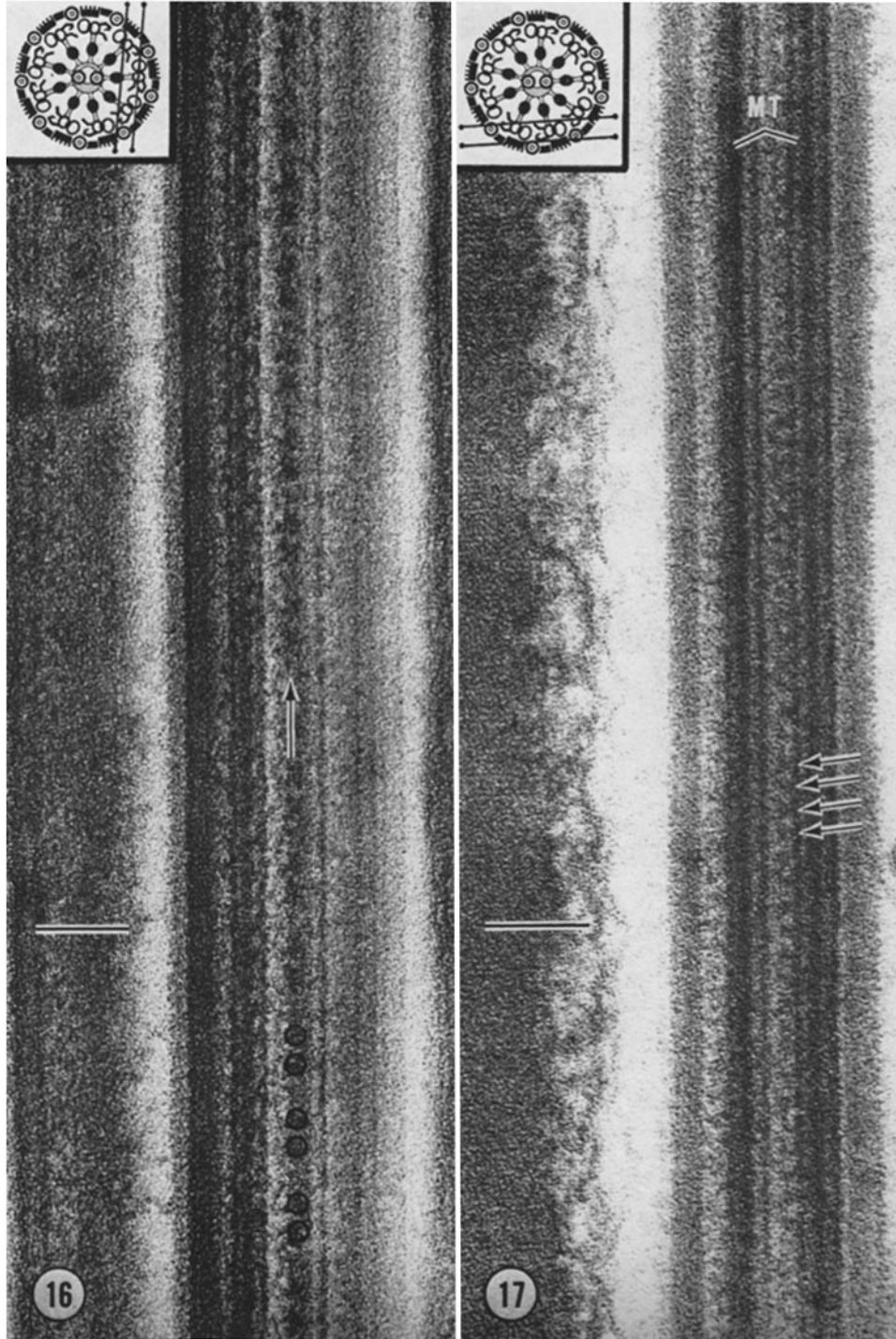
FIGURE 16   Peripheral section passing between the link heads and a doublet such that a row of radial links is transversely sectioned. The links' paired spacing (circles) along the row (arrow) is evident. × 135,000.

FIGURE 17   Peripheral section including two sets of doublet tubules. The A tubule of each doublet is indicated (*MT*). The arms are visible, spaced regularly along one of the doublets (arrows). No connections are visible between the arms and the adjacent doublet. × 150,000.
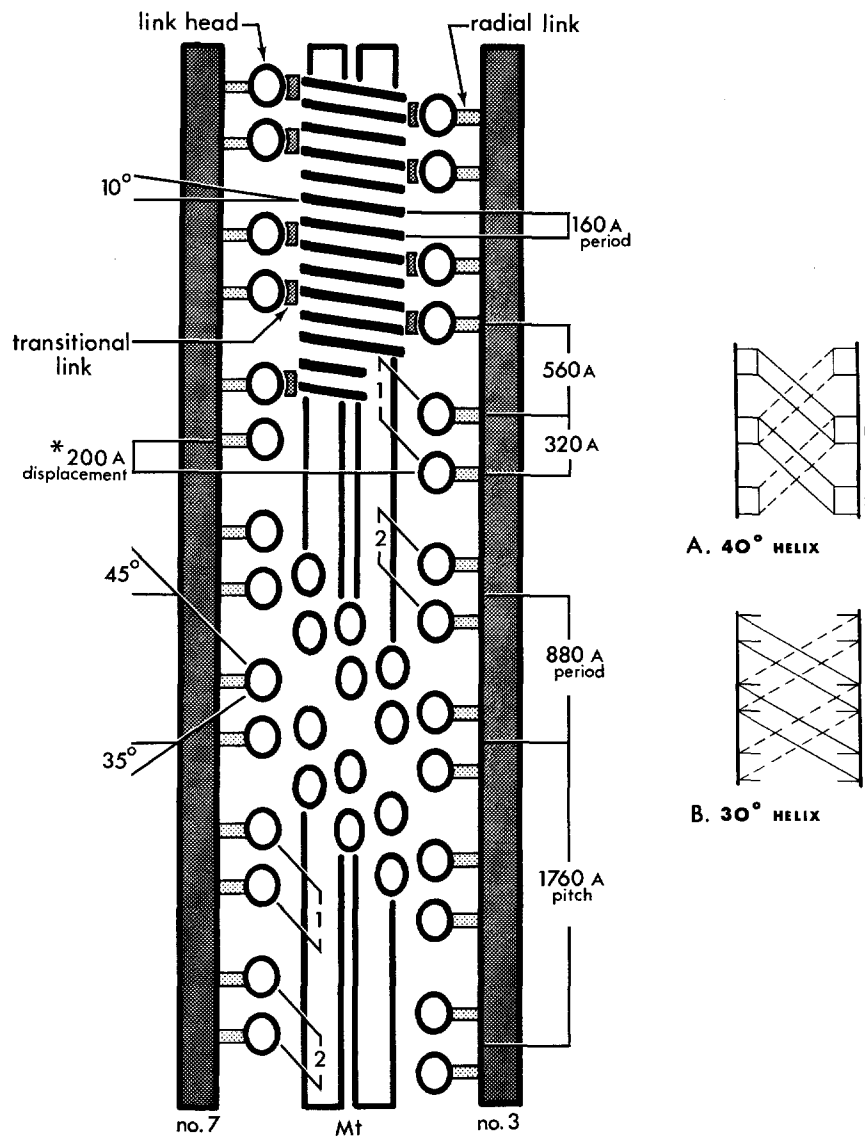
Figure 18 Diagram of the flagellar axoneme as it appears in longitudinal view from several levels of optical section. Coarse fibers, accessory tubules, and arms are omitted. The left-handed, double helical configuration (1, 2) of the link heads is shown winding with alternating half-turn angles of 35° and 45°, due to the *200 A displacement of link heads on opposite sides of the axoneme. The helix of radial links and heads joins the doublet A tubules (7 and 3) to the 160 A sheath striations around the central pair tubules (Mt) via the transitional links. The inserts depict the probable helical organization when opposing links are in register. A., 40° helix drawn at the link head site. B., 30° helix drawn at the link-microtubule wall junction. All figures are drawn approximately to scale.

shows three doublets lying completely on their sides so that three or four subfilaments are visible in the wall of each tubule. The links are transversely superimposed over both tubules and project a short distance past the lateral edge of the B tubule. Their organization is ambiguous when viewed in this plane. The nature of the link-microtubule wall junction is not clear in any of the negatively stained preparations, although the subunits of the tubule wall appear in Fig. 23 as 40 A,
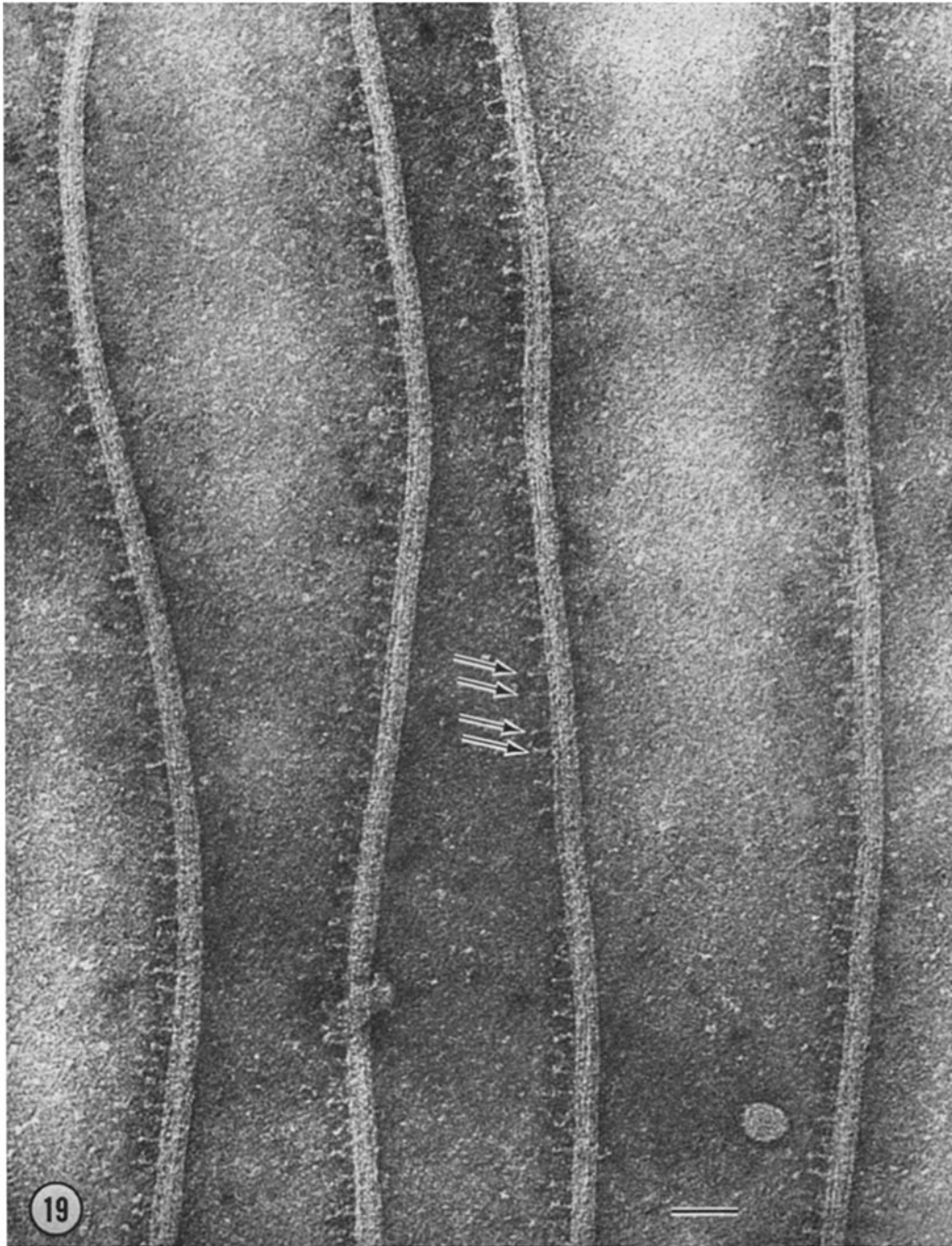
FIGURE 19 PTA negatively stained preparation showing four sets of doublet tubules. Each doublet is lying so that the A and B tubules are superimposed. The paired radial links (arrows) are clearly visible projecting from each doublet. × 96,000.

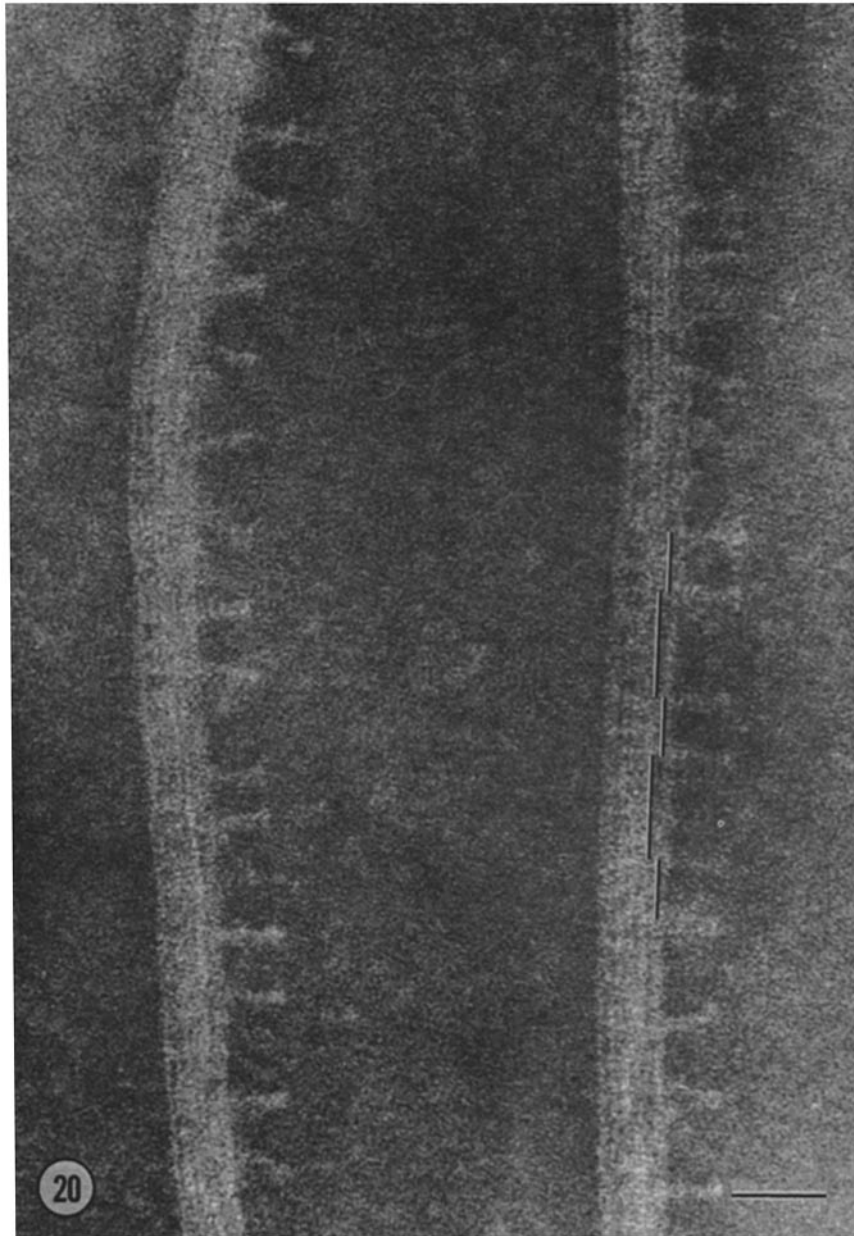FRED D. WARNER *Flagellar Fine Structure* **173**

FIGURE 20   High-magnification view of 2 PTA-stained doublets similar to those in the previous figure. The paired radial links show a spacing of 320/560 A (lines) and appear to consist of globular subunits. The calibration bar represents 500 A. × 250,000.

linearly arranged spherules with a center-to-center spacing of about 50 A.

An additional component appears to lie equidistant between link pairs when viewed in sectioned material. This is visible in both median (Figs. 11, 12) and peripheral (Figs. 14, 15) sec-

tions as a dense region somewhat smaller than the adjacent link heads. It is not clear whether this material is an actual structure or simply represents condensation of the amorphous matrix material between link pairs; however, it does not join with the central sheath as do the link heads.
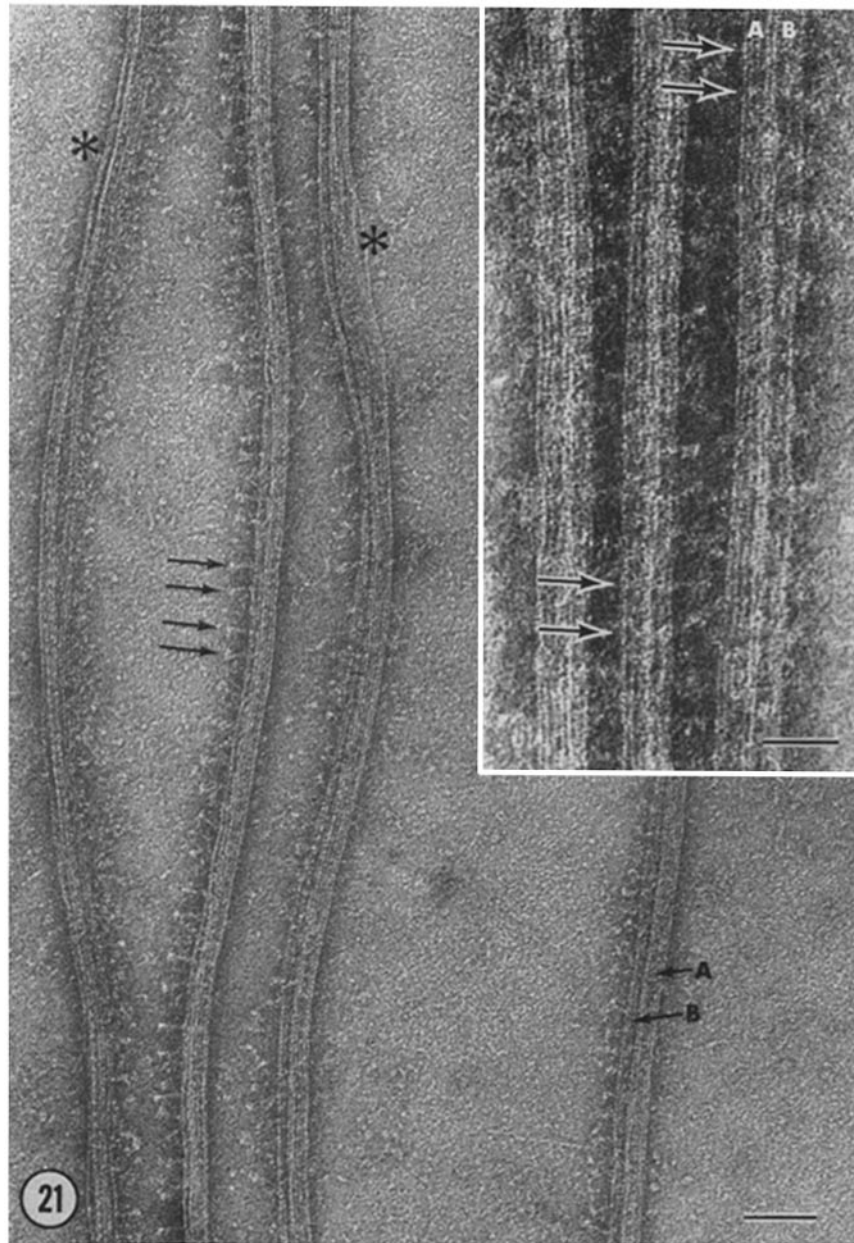
FIGURE 21 PTA negatively stained preparation showing four collapsed doublets with both A and B tubules visible. The radial links are often obscured, but are clear in regions (arrows). Along the doublets indicated by (*), the lack of links is due partially to doublet degradation. × 96,000. The *insert* illustrates three doublets with both A and B tubules clearly visible. The links lie transversely superimposed over each doublet (arrows) and project about 100 A past the lateral edge of the B tubule. The calibration bar represents 500 A. × 200,000.
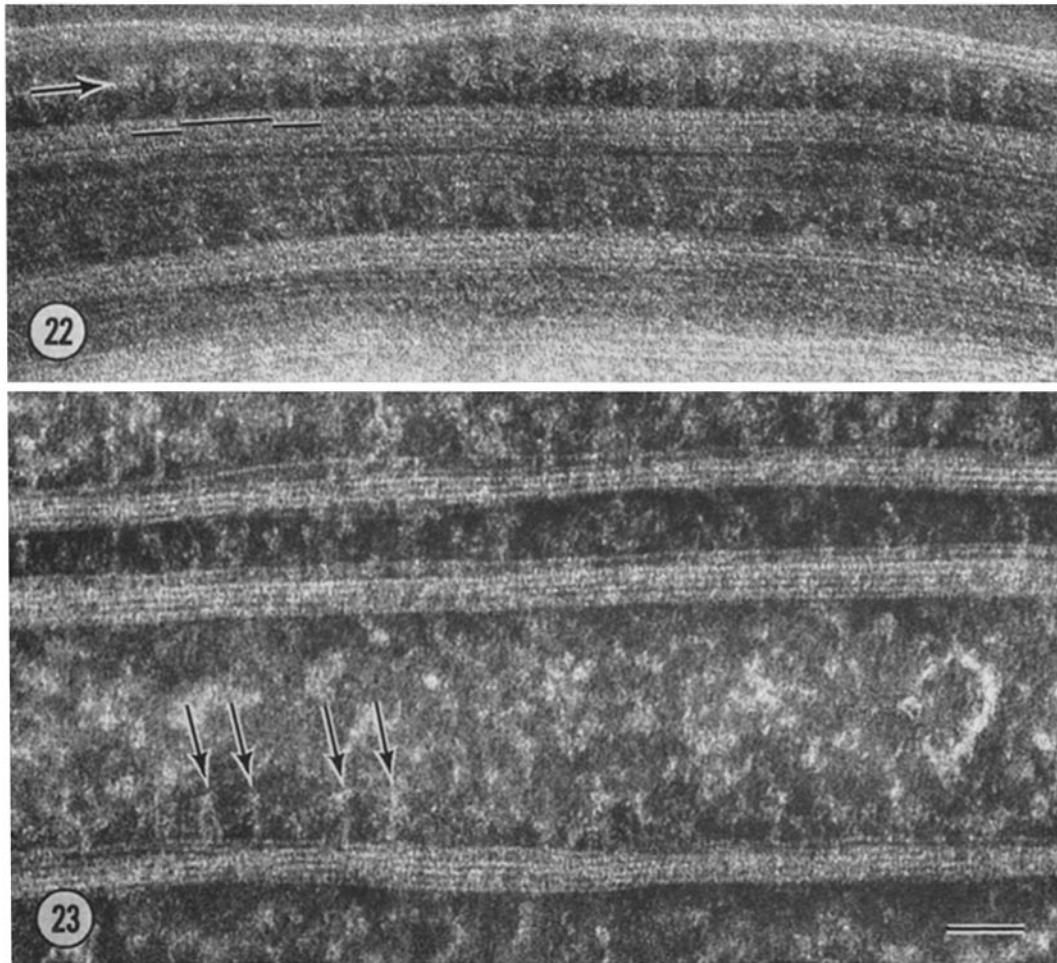
FIGURE 22   Two collapsed doublets negatively stained with PTA. Paired radial links project from the A tubule (lines). The link heads are visible as a row of globules appearing somewhat dispersed in this preparation (arrow). Considerable amorphous material lies between adjacent links. × 200,000.

FIGURE 23   PTA negatively stained preparation showing three partially collapsed doublets. The radial links are generally obscured although a few are visible (arrows). The 40 A subunits comprising the microtubule wall are clear. The calibration bar represents 500 A. × 200,000.

Negatively stained preparations show only amorphous material in this region (Fig. 22).

Transitional Links

In transverse axoneme sections, there are sites of junction between radial link heads and the surface of the central sheath (Fig. 2), although not all link heads show junction in a given section. This region is largely obscured in the rotation images, owing to the lack of ninefold symmetry associated with the central region. In a longi-

tudinal surface section of the sheath, prominent junctional sites often appear (Fig. 10). It is not clear whether this junction represents an additional structural component or whether the head and sheath join directly, although the junction spans a distance of about 100 A. Whenever junctions are visible, it appears that two sheath striations are joined to each head. The junctional region was not preserved in negatively stained preparations. This site is tentatively designated a *transitional link*.

DISCUSSION

The present study has revealed little that is new relative to flagellar microtubule organization. The $9 + 9 + 2$ configuration is typical of many arthropod spermatozoa and probably represents an evolutionary divergence of the $9 + 2$ pattern. However, it is important to note that the nine accessory tubules of some insect sperm appear to be homologous with the c microtubule of the basal boty triplets[1] (22), and their displacement centrifugal to the doublets may reflect the importance of doublet spacing to the motile process.

The site of the ATPase protein "dynein" (13) has been localized in the paired arms along doublet tubule A. The arms are consistent features of motile cilia and flagella showing ninefold symmetry and also appear along the doublets of sciarid sperm flagella (23). As viewed in this study, the arms are spaced at regular intervals of 200–220 A along the A tubule which is in the spacing range as currently observed by Gibbons (personal communication). Since the arms are only rarely observed in negatively stained preparations (16), their precise in situ configuration has yet to be ascertained. Some of the structural parameters are nicely discussed by Allen (2) and Gibbons (14). The presence of links or bridges between adjacent doublets is often reported (2, 12, 26, 28, 34), but no firm evidence of such linkage was observed in Sarcophaga sperm, except for the occasional faint strands connecting the inner arm with the adjacent doublet. Rosenbaum (unpublished observations) observes prominent linkage in preparations of isolated, partially disrupted Chlamydomonas flagella which seems to be holding the doublets together.

Central Sheath

A helical central sheath appears to be a consistent feature of (9) + 9 + 2 cilia and flagella (4, 10, 11, 21, 26, 34) although its precise configuration remains uncertain since the sheath is rarely, if at all, preserved in negatively stained preparations. At this time it cannot be considered as a simple "thread" coiled around the central tubules. In sectioned material, the sheath does not appear to encompass the opposed lateral edges of the tubules although the 160 A tubule period is in register with the sheath period at this site.

Perotti (22) shows illustrations of negatively stained central pair tubules of Drosophila sperm, along which lie regular projections showing a period of 150–170 A. She interprets the projections to be helically disposed around the tubules and suggests that they are related to, or may be, the central sheath. In a recent study by Chasey (9) on Tetrahymena central pair tubules, similar projections occur but apparently along only one of the tubules. These projections show a period of 160 A and were observed to become detached from the tubule wall. Chasey suggests that they may be the projections observed by both Allen (2) and Williams and Luft (34) in thin-sectioned material of Tetrahymena. Similar projections are visible in developmental stages of insect sperm[1] (17) and may represent the forming sheath. In thin sections of Sarcophaga, 160 A periodic striations were observed over both central tubules. These striations are in register with the more centrifugal sheath striations and seem to bridge the gap separating the two tubules on the Y side of the sheath. Whether they are the innermost portion of the sheath cannot be stated. However, both tubule (Fig. 7) and sheath (Fig. 9) striations occur with a 160 A period, are inclined at 8–10° with the same handedness, and are helically disposed. It may be that the projections observed by both Chasey and Perotti represent attachment sites of the sheath to the microtubule wall, and may, in turn, be related to the inherent 160 A period of the tubule wall as described by Grimstone and Klug (15). In any case, research being done by Chasey (personal communication) with optical diffraction techniques should clarify these relationships.

Platyhelminth sperm flagella show an apparent evolutionary divergence in the form of the central region. The central tubules and sheath have been replaced by a central core (8, 31) consisting of helically disposed subunits (32, 36). Silveira (32) has shown that the core periphery consists of a double helix showing a period of 700 A and a subspacing of about 130 A within each strand. She reports that the radial links join with the core helices; hence the relationship appears to be analogous, if not homologous, to the situation in $9 + 2$ flagella. The (9) + 9 + 1_n and (9) + 9 + 0 sperm flagella of some insect species (24) show analogous modifications of the central region, and these appear to be linked in a similar manner to the peripheral doublets.

Radial Link Organization

The presence of nine longitudinal "secondary fibers" was indicated by early studies of ciliary

fine structure (11, 12). They were observed to be positioned midway between doublets and central sheath and appeared to be connected to both by radial projections. These "fibers" were also described by André (4) in insect sperm and have been most recently studied by Birge and Doolin (6) in ciliated embryonic tissue. However, from Perotti's (22) work on *Drosophila* sperm, and from the information presented in this paper and from independent observations on *Chlamydomonas* flagella, it appears unequivocal that the so-called secondary fibers are artefacts produced by linear alignment of the enlarged radial link heads in thick sections. It is clear, from both thin-sectioned and negatively stained material, that there are no structural connections between either linearly or helically adjacent link heads, although amorphous, electron-opaque material is dispersed between linearly adjacent heads. This amorphous material is apparently degraded during fixation of many cilia and flagella but is retained in insect sperm and thus obscures the radial links while giving the impression that the link head rows are a continuous fiber. For comparison purposes, a single *Chlamydomonas* flagellum is illustrated in Fig. 24. The matrix region is extracted, but the paired radial links are quite clear.

The radial links as demonstrated in this study correspond to the "spokes" as first described by Afzelius (1). The term *radial link*, as used by Gibbons (12), more accurately denotes both the structure and organization of these units and is thus adopted. The links have been conclusively demonstrated for the first time in *Sarcophaga* spermatid flagella, by the use of both thin-sectioned and negative staining techniques. Perotti (22) has recently described similar links in *Drosophila* sperm. However, from a perusal of past work, it is clear that the radial projections often appeared in negatively stained preparations. For example, Behnke and Forer (reference 5, Fig. 23) include an excellent micrograph of the paired links, with globular heads intact, along the doublet tubules of crane-fly spermatids, although the authors were uncertain as to whether they were radial links or the dynein arms. Similarly, Burton (reference 8, Fig. 20) shows the links in lung-fluke spermatozoa. The links have also been observed in negatively stained *Tetrahymena* cilia (Chasey, personal communication) and consistently appear in both sectioned (Fig. 24) and negatively stained *Chlamydomonas* flagella (Hopkins, unpublished results). The
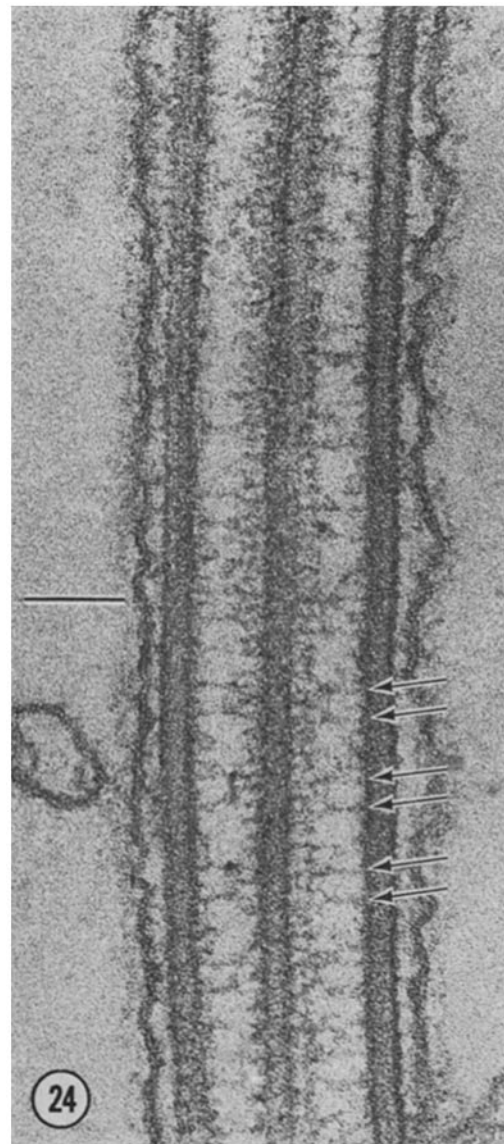

FIGURE 24   Longitudinal section through a flagellum of *Chlamydomonas reinhardi*. Paired radial links are visible connecting the doublets with the central sheath (arrows). The link heads are much smaller in this material, and the matrix region is extracted so that the link organization is clear. Link spacing on both sides of the axoneme is about 320/640 A. The calibration bar represents 1000 A. Glutaraldehyde-phosphate-osmium tetroxide fixation. × 133,000.

visualization of the links in a variety of organisms seems to depend on the degree of matrix extraction caused by the preparative procedures. In negatively stained flagella, the links are most often ob-

served when the doublets are well spread and have fallen such that the A and B tubules are superimposed

An interesting feature of the radial links is their paired spacing along the doublet wall. In averaged measurements taken from the published micrographs, links are spaced at 320/640 A in crane-fly sperm (5); 320/560, 640 A in *Drosophila* sperm (22); 320/640 A in lung-fluke sperm (8); 320/640 A in *Chlamydomonas* flagella (personal observations); and 320/560, 640 A in *Sarcophaga* spermatids. All of these spacings are even multiples of one or more of the 40, 80, or 160 A inherent periods of the flagellar microtubule wall (15). High-resolution micrographs showing irregular link spacings appear in the literature (26, 34); however, these must be carefully interpreted since the maximum distance separating any two doublets and their links in thin-sections is ca. 300 A. Hence, superimposition of adjacent link rows could occur and, owing to the links' helical disposition, an irregular period might result. There are good indications that link groupings other than paired groupings occur. Gibbons (personal communication) tentatively finds links in groups of three with a repeating period of about 1000 A in sectioned *Tetrahymena* cilia, while Chasey (personal communication) observes a similar triplet grouping in negatively stained preparations. Similarly, Satir and Gilula (personal communication) observe a single link repeating at about 900 A in *Elliptio* gill cilia.

An intriguing aspect of link organization is the helical disposition of links in the flagellar matrix. The first indication of such organization was reported by Manton and Clarke (19) in partially fragmented *Sphagnum* sperm flagella. Silveira and Porter (31) and Silveira (32) inferred helical disposition of the links in platyhelminth sperm. Paolillo (21) recently observed a double helix in the matrix of *Polytrichum* sperm flagella. The helix has a pitch of about 1500 A and an angular inclination of about 35° (my measurements). Paolillo suggests that five subunits (link heads?) make up each strand of the helix, although resolution did not permit a precise analysis. Paolillo and Manton and Clarke interpreted the helix as a real structure rather than a mode of organization. A structural helix linked to the peripheral doublets would be inconsistent with what is now known about flagellar bending and microtubule sliding (see below).

Sarcophaga spermatids demonstrate the presence of a double helix in form only, not in helically linked structure. Each strand of the helix is visualized by the paired link heads which wind with half-turn angles of approximately 40° down the flagellar matrix, probably in a left-handed fashion although this was not conclusively determined. Perotti (22) describes a similar helix in *Drosophila* sperm which she interprets to be an alternating right, left-handed helix with a 30° inclination at the doublet tubule-link junction. In the present study, figures showing angular alignment of link head pairs (Figs. 12, 14, 15) do not completely exclude the possibility of planar link organization rather than helical. If the links were planar, the passive bending occurring along the flagellum (see below) might still produce angular alignment similar to that illustrated. However, planar organization could still be detected in certain peripheral sections, regardless of flagellar bending and doublet sliding. Satir has indicated (reference 30, Fig. 10) that the ciliary stroke plane in *Elliptio* is slightly asymmetric and lies near doublets [4, 5] (effective) and [6, 7] (recovery). Thus he observed no measurable sliding between the two doublets in each group since their position relative to one another does not change during the stroke pattern. Accordingly, if link organization were planar, any peripheral section showing laterally adjacent link heads from doublets in the effective bend plane should show the head pairs in perfect transverse register. This was not observed in *Sarcophaga*. All peripheral sections examined (~60, all possible planes) show a minimum head pair displacement of about 170 A, as would be expected for a 40° helix of link heads (see next section).

Should there be any doubt as to the nature of link disposition, Paolillo (reference 21, Fig. 7) shows an interesting micrograph that traverses the axoneme diameter in longitudinal section. On one side, the helix inclination is from left-to-right, but as the section plane crosses to the opposite side there is an abrupt reversal of inclination.

Helix Distortion and Microtubule Sliding

Presuming that helical organization must be symmetrical through successive half-turns, and given a constant period and pitch, we must consider the nature of the 25–55° inclination angles and 160–440 A link head displacements observed

in the matrix. Due to the inherent asymmetry of doublets and links, any median section of the axoneme will show a maximum displacement of 196 A for opposed link head pairs, irrespective of doublet sliding. That is, a median section is not a perfect bisection of the helix, and thus the 196 A helical displacement of head pairs necessitated by a 40°, 1760 A helix pitch angle will be apparent as a distorted helix. However, this does not account for the 440 A maximum displacement observed in both median and peripheral sections.

As noted at the beginning of the Results section, the flagellum does not lie straight within the testes but assumes the form of numerous passive bends. Accordingly, passive doublet sliding must have occurred along much of the flagellar length, thus resulting in helix distortion. Satir (29, 30) has shown that in a cilium showing a single bend, doublet sliding is initiated at the bend and translated distally to the tip in order to accommodate the bend curvature. Because the bend is perpendicular to the central tubule plane, predicted values of doublet sliding form two half-circle gradients around the axoneme. Maximum and minimum sliding values thus occur in the bend plane or between doublet groups [5, 6] and [9, 1, 2]. Since the spermatid flagella used in this study show several bends along their length, partial recovery of doublet sliding must have occurred in regions (33). The 25–55° angles observed are consistent with about 0–440 A of doublet sliding beyond the o position or 40° link head inclination. However, this does not indicate the true linear extent of sliding between any two doublets. In median section, the helix will appear to have become reorganized to the 40° position with every frameshift of the period or 880 A since opposed link heads will again lie in register. Thus, the maximum amount of sliding that can be detected in median sections of the axoneme is 440 A or one-half the helix period. Satir (30) has observed maximum doublet sliding (Δl_n) of about 4000 A between opposed doublets and about 1000 A between adjacent doublets.

Satir (29) earlier suggested that a bend is initially restricted to its point of origin near the ciliary base. He shows that the arc length for a bend of angle 51° and minimum radius of curvature is 1.78 μ. As maximum distortion of this 1.78 μ bend unit is reached, owing to presumed contractile elements, a second unit is triggered and so on, thus translating the bend to the cilium

tip. Maximum distortion of the bend unit was predicted when doublet sliding (Δl) of 1790 A was achieved, a figure equivalent to the 1760 A helix pitch observed in this study. In order to account for the observed 1790 A of doublet sliding, Satir then predicted sliding to occur as a result of quantum displacements of 175 A within the bend unit. The maximum number of such displacements in the 1.78 μ bend is thus $\sim$10. The 175 A displacement is the same as the dynein arm spacing as observed by Satir, but is also in the range of the central sheath period (see below). In *Sarcophaga* spermatids, it seems reasonable to suggest that the maximum sliding distortion of the link helix is in the order of the pitch or 1760 A. Doublet sliding beyond the pitch value would seem to require helix reorganization and/or triggering of another bend unit if a stable helical matrix organization is to be maintained.

These relationships to Satir's observations may be coincidental or may be directly related to the motile mechanism. The observed helix angular distortion assumes that radial link attachment to the A tubule wall is fixed, and preliminary studies of bent regions indicate that this is true. Thus, when doublet sliding occurs, it must be accompanied by concomitant displacement of link heads along the surface of the central sheath. The presence of linkage, here termed transitional links, between the sheath and link heads is evident in many fine structure studies (6, 10, 21, 26, 34). In insect spermatids (4, present study) linkage appears, although irregularly. This may result from their having been fixed in the inactive state. The organelles in previous studies show consistent linkage and must be regarded as having been fixed while the organelle was motile. In most cases, linkage appears to involve two sheath striations per link head. This suggests that any head displacement due to either sliding or bending must occur in minimum steps of the sheath period or 160 A.

CONCLUSION

The view of flagellar organization that has emerged is far more complex than shown by early observations of the prominent tubule groupings. If we ignore structural variations lying centrifugal to the peripheral doublets, it appears that a similar microtubule-matrix organization may exist in all motile cilia and flagella showing nine-

fold symmetry. Most detailed fine structure studies have suggested such a similarity of organization. Several possible exceptions have been reported (20, 35, 36) which lack obvious structure within the doublet profile, even though the flagella are apparently motile. However, these studies are based on sectioned material alone and need to be corroborated by both high-resolution sectioned and negatively stained preparations. True exceptions to the organization described in this study will be critical to an analysis of ciliary motility. Assuming the self-assembly nature of matrix components, their helical disposition is not surprising since helicity is a feature of microtubule substructure (16) and is the most common form taken by a linear self-assembly system (18). Reedy (25) has demonstrated the helical conformation of striated muscle fiber cross-bridges.

Although the nature of the motile mechanism remains enigmatic, cross-bridging between adjacent doublets and bridging between doublets and central sheath must figure prominently in the mechanism. In the context of doublet sliding (30), any such bridging must be either broken or displaced. Owing to the linear extent of sliding, displacement must lie beyond the range of simple distortion. It is interesting that Anderson and Personne (3) have recently localized intra-axonemal glycogen in the sperm flagella of certain gastropods. The deposits are often symmetrically positioned at the link head site and presumably serve as an endogenous energy source. Biochemical analyses of tubule and matrix fractions should serve in part to elucidate the motile mechanism. It is encouraging to note that J. Rosenbaum (personal communication) currently observes 8–12 protein bands on polyacrylamide gels of *Chlamydomonas* flagellar matrix fraction.

REFERENCES

1. AFZELIUS, B. 1959. *J. Biophys. Biochem. Cytol.* **5**:269.
2. ALLEN, R. D. 1967. *J. Cell Biol.* **37**:825.
3. ANDERSON, W. A., and P. PERSONNE. 1970. *J. Cell Biol.* **44**:29.
4. ANDRÉ, J. 1961. *J. Ultrastruct. Res.* **5**:86.
5. BEHNKE, O., and A. FORER. 1967. *J. Cell Sci.* **2**:169.
6. BIRGE, W. J., and P. F. DOOLIN. 1969. *J. Microsc.* **8**:167.
7. BROKAW, C. J. 1968. *In* Aspects of Cell Motility. *Soc. Exp. Biol. Symp.* Academic Press Inc., New York. **22**:101.
8. BURTON, P. R. 1966. *J. Morphol.* **120**:397.
9. CHASEY, D. 1969. *J. Cell Sci.* **5**:453.
10. FRIEND, D. S. 1966. *J. Cell Biol.* **29**:317.
11. GIBBONS, I. R., and A. V. GRIMSTONE. 1960. *J. Biophys. Biochem. Cytol.* **7**:697.
12. GIBBONS, I. R. 1961. *J. Biophys. Biochem. Cytol.* **11**:179.
13. GIBBONS, I. R. 1965. *Arch. Biol.* **76**:317.
14. GIBBONS, I. R. 1967. *In* Formation and Fate of Cell Organelles. K. B. Warren, editor. Academic Press Inc., New York. 99.
15. GRIMSTONE, A. V., and A. KLUG. 1966. *J. Cell Sci.* **1**:351.
16. HOOKES, D. E., SIR JOHN RANDALL, and J. M. HOPKINS. 1967. *In* Formation and Fate of Cell Organelles. K. B. Warren, editor. Academic Press Inc., New York. 115.
17. KESSEL, R. G. 1967. *J. Ultrastruct. Res.* **18**:677.
18. KLUG, A. 1967. *In* Formation and Fate of Cell Organelles. K. B. Warren, editor. Academic Press Inc., New York. 1.
19. MANTON, I., and B. CLARKE. 1952. *J. Exp. Bot.* **3**:265.
20. MANTON, I., and H. A. VON STOSCH. 1966. *J. Roy. Microsc. Soc.* **85**:119.
21. PAOLILLO, D. J. 1967. *Trans. Amer. Microsc. Soc.* **86**:428.
22. PEROTTI, M. E. 1969. *J. Submicrosc. Cytol.* **1**:171.
23. PHILLIPS, D. M. 1966. *J. Cell Biol.* **30**:499.
24. PHILLIPS, D. M. 1969. *J. Cell Biol.* **40**:28.
25. REEDY, M. K. 1968. *J. Mol. Biol.* **31**:155.
26. RINGO, D. L. 1967. *J. Cell Biol.* **33**:543.
27. ROSS, J., and W. G. ROBISON. 1969. *J. Cell Biol.* **40**:426.
28. SATIR, P. 1965. *J. Cell Biol.* **26**:805.
29. SATIR, P. 1967. *J. Gen. Physiol.* **50**:241.
30. SATIR, P. 1969. *J. Cell Biol.* **39**:77.
31. SILVEIRA, M., and K. R. PORTER. 1964. *Protoplasma.* **59**:240.
32. SILVEIRA, M. 1969. *J. Ultrastruct. Res.* **26**:274.

33. SLEIGH, M. A. 1968. *In* Aspects of Cell Motility. *Soc. Exp. Biol. Symp.* Academic Press Inc., New York. **22**:131.

34. WILLIAMS, N. E., and J. H. LUFT. 1968. *J. Ultrastruct. Res.* **25**:271.

35. AFZELIUS, B. A. 1969. *In* Handbook of Molecular Cytology. A. Lima-de-Faria, editor. North-Holland Publ. Co., Amsterdam. 1219.

36. HENLEY, C., D. P. COSTELLO, M. B. THOMAS, and W. D. NEWTON. 1969. *Proc. Nat. Acad. Sci. U. S. A.* **64**:849.

37. HOLWILL, M. E. J. 1966. *Physiol. Rev.* **46**:696.